J. Gorosabel *et al.*, in preparation.
21. P. Mészáros and M. J. Rees, *Astrophys. J.* **405**, 278 (1993); *ibid.* **418**, L59 (1993).
22. ———, *ibid.* **476**, 232 (1997).
23. The impulsive fireball model in (*22*) predicts that the observed break frequency ν_m crosses the optical band at a time $t_{op} \sim 3 \times 10^3\ t_\gamma$, where t_γ is the duration of the gamma ray flash. Taking into account that the bulk of the GRB 970508 gamma ray emission lasted 3.6 s, $t_{op} \sim 3$ hours, which is much shorter than the observed $t_{op} \sim 2$ days.
24. R. A. M. J. Wijers, M. J. Rees, P. Mészáros, *Mon. Not. R. Astron. Soc.* **288**, L51 (1997)
25. J. I. Katz and T. Piran, *Astrophys. J.* **490**, 772 (1997); and references therein.
26. Like GRO J0422+32 [A. J. Castro-Tirado, J. L. Ortiz, J. Gallego, *Astron. Astrophys.* **322**, 507 (1997)] and GRO J1655-40 [J. A. Orosz, R. A. Remillard, Ch. D. Bailyn, J. E. McClintock, *Astrophys. J.* **478**, L83 (1997)].
27. S. K. Chakrabarti and P. J. Wiita, *Astrophys. J.* **411**, 602 (1993). See also J. J. Brainerd, *ibid.* **394**, L33 (1992).
28. M. Vietri, *ibid.* **488**, L105 (1997).
29. The fastest x-ray flare ever seen in an extragalactic object was observed in May 1994 in the BL Lac object PKS 2155-304. The x-ray flare was followed by a broader, lower amplitude extreme-UV flare ~1 day later and a broad, low-amplitude UV flare ~2 days later [E. Pian *et al.*, *Astrophys. J.* **486**, 784 (1997)].
30. M. Tavani, *Astrophys. J.* **466**, 768 (1996); E. Waxman, *ibid.* **485**, L5 (1997).
31. T. Galama *et al.*, *IAU Circ. 6655* (1997).
32. M. R. Metzger *et al.*, *IAU Circ. 6676* (1997).
33. S. Djorgovski *et al.*, *IAU Circ. 6658* (1997); *IAU Circ. 6660* (1997); B. Schaefer *et al.*, *IAU Circ. 6658* (1997); P. Groot *et al.*, *IAU Circ. 6660* (1997); C. Chevalier and S. Ilovaisky, *IAU Circ. 6663* (1997); A. Kopylov *et al.*, *ibid.*; *IAU Circ. 6671* (1997); A. Fruchter and L. Bergeron, *IAU Circ. 6674* (1997); (*31, 32*).
34. We are grateful to M. Santos-Lleó, M. Más-Hesse, B. Montesinos, P. Rodríguez-Pascual, L. Sánz Fernández de Córdoba, E. Fernandes-Vieira, J. R. Acarreta, A. Alberdi, M. Cerviño, T. Galama, N. Schartel, D. Thompson, and R. Wijers for fruitful conversations, and to J. Gallego, J. Zamorano, and M. Fernández for their good will. We are grateful to the director of NOT for his continued support of this program, and to J. Perez-Mercador for his encouragement. J. Greiner is supported by the Deutsche Agentur für Raumfahrtangelegenheiten. C.B., A.G., N.M., and A.P. acknowledge the support of the Università di Bologna. The BeppoSAX team acknowledges the Italian Space Agency for support. The Calar Alto German-Spanish Observatory is operated jointly by the Max-Planck Institut für Astronomie in Heidelberg and the Comisión Nacional de Astronomía, Madrid. The WHT is operated by the Royal Greenwich Observatory in the Spanish Observatorio del Roque de los Muchachos of the Institutò de Astrofísica de Canarias. The Loiano Telescope is operated by Osservatorio Astronomico di Bologna and Università di Bologna.

24 June 1997; accepted 14 January 1998

Temperature and Surface-Ocean Water Balance of the Mid-Holocene Tropical Western Pacific

Michael K. Gagan, Linda K. Ayliffe, David Hopley, Joseph A. Cali, Graham E. Mortimer, John Chappell, Malcolm T. McCulloch, M. John Head

Skeletal Sr/Ca and $^{18}O/^{16}O$ ratios in corals from the Great Barrier Reef, Australia, indicate that the tropical ocean surface ~5350 years ago was 1°C warmer and enriched in ^{18}O by 0.5 per mil relative to modern seawater. The results suggest that the temperature increase enhanced the evaporative enrichment of ^{18}O in seawater. Transport of part of the additional atmospheric water vapor to extratropical latitudes may have sustained the $^{18}O/^{16}O$ anomaly. The reduced glacial-Holocene shift in seawater $^{18}O/^{16}O$ ratio produced by the mid-Holocene ^{18}O enrichment may help to reconcile the different temperature histories for the last deglaciation given by coral Sr/Ca thermometry and foraminiferal oxygen-isotope records.

Oxygen isotopes in foraminifera from deep-sea cores have been used successfully to reconstruct continental ice volumes, glacio-eustatic sea level, and deep-ocean temperatures throughout the last glacial-interglacial cycle (*1*). Yet there is still considerable debate regarding the relative contributions of changes in the oxygen isotopic composition of seawater and ocean temperature to the change in foraminiferal $\delta^{18}O$ values (*2*) in the tropical surface ocean. The amplitude of the glacial-Holocene $\delta^{18}O$ shift for planktonic foraminifera in the tropics is about the same as that for foraminifera living in the near-constant temperature environment of the deep ocean (*3*). The apparent similarity between the two records has led to the interpretation that the tropical surface ocean cooled by no more than 2°C during the last glacial maximum (LGM), an interpretation reinforced by the conclusions of the CLIMAP project (*4*). Recent measurements of Sr/Ca ratios in corals from Barbados (*5*) and Vanuatu (*6*) indicate that both the tropical Atlantic and Pacific oceans cooled by up to 5°C during the LGM. Despite the consistency of this cooling with the 5°to 8°C cooling estimated for the tropical atmosphere (*7*), the coral records have not been widely accepted because the glacial-Holocene $\delta^{18}O$ shift recorded by planktonic foraminifera cannot accommodate an ocean temperature shift of 5°C, particularly in the tropical Pacific where the $\delta^{18}O$ shift is anomalously small (*8*). If the coral Sr/Ca thermometer is reliable, the relatively small $\delta^{18}O$ shift for Pacific planktonics may be a result of undetected changes in the distribution of ^{18}O in the surface ocean (*9*). Therefore, obtaining accurate estimates of the past ^{18}O distribution in tropical surface waters, by some independent means, is crucial to establishing the role of the tropical oceans in global climate change.

In principle, precise measurements of Sr/Ca ratios and $\delta^{18}O$ values in coralline aragonite should make it possible to determine uniquely the past oxygen isotopic composition of seawater, by removal of the temperature component of the coral $\delta^{18}O$ signal. However, the temperature dependence of coral Sr/Ca ratios has been questioned recently (*10*) on the basis that biological controls on Sr and Ca uptake can induce uncertainties of up to 3°C in reconstructed temperatures. Here, we first verify the reliability of the coral Sr/Ca thermometer for several modern corals growing in suboptimal environmental settings like those that may prevail during glacial-interglacial transitions when corals colonize transient shorelines marked by fluctuations in temperature, salinity, and water turbidity. Next we demonstrate a strong correlation between coral Sr/Ca and $\delta^{18}O$ and, by coupling these measurements, determine the surface temperature and $\delta^{18}O$ of western Pacific seawater soon after the end of the last deglaciation. Interpretations of the glacial-Holocene shift in foraminiferal $\delta^{18}O$ have been made with the assumption that the ^{18}O distribution in the surface ocean was the same as today at ~6000 years before the present, by which time the discharge into the ocean of ^{18}O-depleted polar meltwater was essentially complete (*11*). We test this assumption by analyzing a 5350-year B.P. coral from the Great Barrier Reef.

We measured skeletal Sr/Ca (*12*) for colonies of *Porites lutea* growing in three different oceanic environments including the Great Barrier Reef, the eastern Indian Ocean, and the Indonesian seaway. These test sites encompass seasonal sea surface temperature (SST) ranges (20° to 31°C) spanning much of the survival range for

M. K. Gagan, L. K. Ayliffe, J. A. Cali, G. E. Mortimer, M. T. McCulloch, Research School of Earth Sciences, Australian National University, Canberra, ACT 0200, Australia.
D. Hopley, Sir George Fisher Centre, James Cook University, Townsville, Queensland 4811, Australia.
J. Chappell and M. J. Head, Research School of Pacific and Asian Studies, Australian National University, Canberra, ACT 0200, Australia.

Porites and cover the entire range of SSTs defined by fossil corals for the last deglaciation (*5*, *6*). Moreover, the corals are exposed to seasonal extremes in salinity (28 to 39 per mil), coastal upwelling, and changes in water column turbidity, all of which might affect the uptake of Sr and Ca by coral skeletons (*13*) (Table 1). We took several precautions to avoid systematic errors in comparing skeletal Sr/Ca data among corals and in comparing coral data with instrumental data (*14*). We matched the coral Sr/Ca ratios and instrumental SST records (*15*) by first converting the coral data to an accurate time series, as described (*16*) (Fig. 1). We then performed least-squares regressions of coral Sr/Ca ratios and instrumental SSTs using the data points defining the temperature maxima and minima for each coral record, totaling 16 years. The average difference between the three Sr/Ca-SST regression equations and their mean is 0.3°C over the entire SST range of 20° to 31°C (Fig. 2). As a result, the mean of the three regression equations justifiably provides a single Sr/Ca-SST relation for *P. lutea* defined by $T = 168.2 - [15{,}674\ (\mathrm{Sr/Ca})_{\mathrm{atomic}}]$. This relation is essentially the same as the original equations derived by Smith *et al.* (*17*) and Beck *et al.* (*12*) and, above 26°C, the relation matches more recent calibrations for *P. lutea* and *P. lobata* (*18*). Differences of up to 3°C between these relations and others derived for the genus *Porites* (*13*, *19*) remain to be resolved.

To assess the effect of calcification rate on skeletal Sr/Ca ratios and $\delta^{18}O$ values (*20*), we examined two *P. lutea* specimens growing at different rates in the same reef environment at Orpheus Island, central Great Barrier Reef. The mean annual extension rates (12 and 22 mm year^{-1}) and calcification rates (1.3 and 2.5 g cm^{-2} year^{-1}) (*21*) span a large portion of the spectrum of growth rates reported for *Porites* (*22*). The degree of correlation between the

Table 1. Summary of study site locations, range of coral growth rates, and attributes of suboptimal growth environments for *P. lutea*.

Location	Extension (mm year^{-1})	Density (g cm^{-3})	Calcification (g cm^{-2} year^{-1})	SST (°C)	Salinity (per mil)	Environment
Nusa Barung Island, Java	24	1.17	2.8	20 to 30	30 to 34	Monsoonal rainfall, coastal upwelling
Orpheus Island, central GBR	22 12.5	1.15 1.08	2.5 1.3	22 to 29	28 to 36	Monsoonal river runoff
Dampier Archipelago, eastern Indian Ocean	8	1.13	0.9	20 to 31	35 to 39	Seasonal hypersalinity

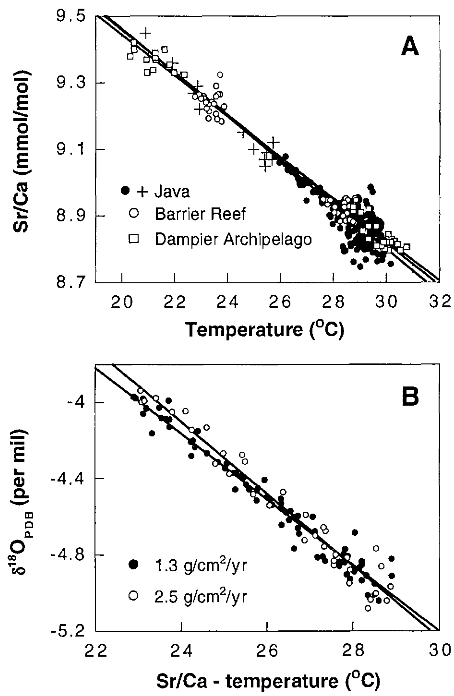

Fig. 2. (**A**) Linear relations between coral Sr/Ca and temperature for *P. lutea* colonies living in environments that are suboptimal for coral growth. Regression lines are calculated with data points defining the temperature maxima and minima of each data set, as defined in Fig. 1. Sr/Ca ratios for the Java coral corresponding to SSTs <26°C (+) are regressed against temperatures derived by ATSR (*37*). The [Sr/Ca]-temperature (*T*) regression lines are $10^3[\mathrm{Sr/Ca}]_{\mathrm{Java}} = 10.78 - 0.0660T$ (r = 0.80); $10^3[\mathrm{Sr/Ca}]_{\mathrm{Orpheus}} = 10.73 - 0.0639T$ (r = 0.98); and $10^3[\mathrm{Sr/Ca}]_{\mathrm{Dampier}} = 10.68 - 0.0616T$ (r = 0.99). (**B**) Comparison of the relation between coral Sr/Ca-derived SSTs and $\delta^{18}O$ for two *P. lutea* colonies calcifying at different rates in the same reef environment at Orpheus Island, central Great Barrier Reef. The regression lines are $[\delta^{18}O]_{1.3\,\mathrm{g\ cm^{-2}year^{-1}}} = 0.002 - 0.174T$ (r = 0.98) and $[\delta^{18}O]_{2.5\,\mathrm{g\ cm^{-2}year^{-1}}} = 0.447 - 0.189T$ (r = 0.98), where Sr/Ca-temperature is defined by the mean of the three coral Sr/Ca-temperature relations.

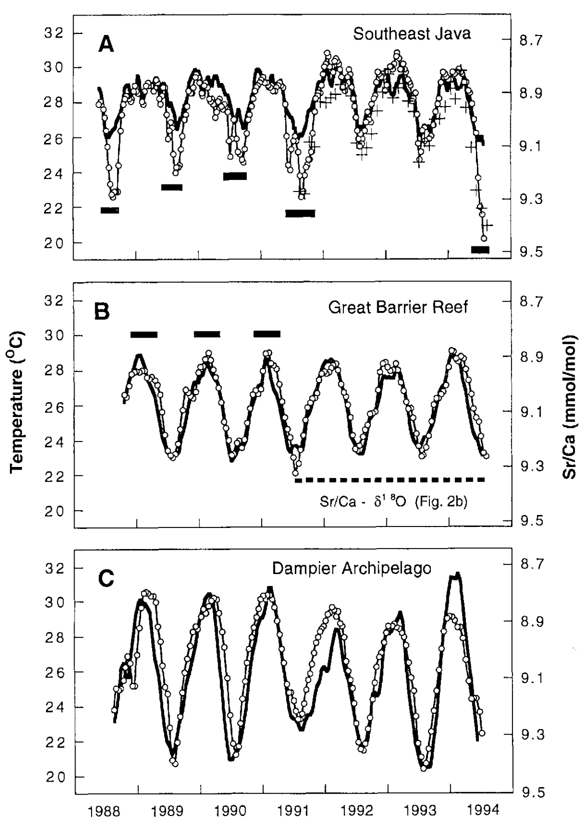

Fig. 1. (**A** to **C**) Comparison between coral Sr/Ca in *P. lutea* (O) and blended ship- and satellite-derived SSTs (solid curves) (*15*) for Nusa Barung Island, southeast Java (8°31′S, 113°22 E); Orpheus Island, central Great Barrier Reef (18°45′S, 146°29′E); and Dampier Archipelago, eastern Indian Ocean (20°36′S, 116°45′E). The Dampier coral grew in shallow nearshore waters where the seasonal range in SST is larger than that recorded by the 1° latitude-longitude grids of the satellite-derived SSTs. Therefore, we adjusted the satellite SSTs for Dampier based on the high degree of covariation observed with an in situ SST record spanning 1983 to 1986 where $T_{\mathrm{in\ situ}} = 1.67T_{\mathrm{satellite}} - 18.67$ (r = 0.95). Strong wind-induced upwelling confined to the southern coast of Java produces cooler SSTs during the austral winter that are not recorded by the satellite-derived SSTs, due to the 1° spatial smoothing of these data. We verify the anomalously cool SSTs recorded by the coral in 1991 and 1994 using monthly averaged SSTs (+) derived from new along-track scanning radiometer (ATSR) data averaged over 0.5° latitude-longitude grids (*37*). Bars indicate periods when upwelling (A) and freshwater runoff from mainland rivers (B) could potentially alter seawater Sr/Ca and reconstructed SSTs. The dashed line in (B) spans the drought of 1992 to 1994 used to establish the correlation between coral Sr/Ca and $\delta^{18}O$ (Fig. 2B).

calibrated coral Sr/Ca temperatures and the $\delta^{18}O$ values can be confirmed during the drought years of 1992 to 1994, which were marked by stable seawater salinities, and presumably stable seawater $\delta^{18}O$ values (Fig. 1). The correlation between the coral Sr/Ca and $\delta^{18}O$ during these years is excellent; the average difference is 0.3°C between the two regression equations and their mean, despite the twofold difference in calcification rate (Fig. 2). The mean of the two $\delta^{18}O$-SST relations derived by comparison with the coral Sr/Ca-SSTs agrees with an earlier $\delta^{18}O$-SST relation derived for *P. lutea* and *P. lobata* (*23*). The result indicates that consistent Sr/Ca-SST and $\delta^{18}O$-SST relations can be derived for massive *Porites* colonies that are largely independent of calcification rate.

We applied these calibration equations to skeletal Sr/Ca and $\delta^{18}O$ measurements for a fossil *Porites* colony growing in the central Great Barrier Reef, Australia, to determine the SST and oxygen isotopic composition of seawater soon after the end of the last deglaciation. Measurements were made on the basal section of a core 1.5 m long, 76 mm in diameter drilled through the center of a *Porites* micro-atoll 6 m in diameter. The core spans 99 years of continuous coral growth and has a mean radiocarbon age (*24*) of 5350 ± 190 yr B.P. (2σ). We compared the fossil coral data directly with the calibration data for the two modern *Porites* specimens growing in the same open-water reef environment on the windward side of Orpheus Island. Several precautions were taken to ensure the modern and fossil coral data are comparable (*25*). Because of the long residence times of Sr and Ca in ocean water (*12*), errors in the paleotemperature reconstructions for well-preserved mid-Holocene corals should be about the same as those associated with comparisons among modern corals.

The paleotemperature indicated by the fossil coral Sr/Ca record shows that the mean SST ~5350 years ago was 27.0°C, which is 1.2°C warmer than the mean SST for the early 1990s (Fig. 3). Terrestrial pollen and tree-line elevation records elsewhere in the tropical southwest Pacific indicate that the climate was generally warmer from 7000 to 4000 yr B.P. (*26*), consistent with our finding. The difference between the Sr/Ca and $\delta^{18}O$ curves (Fig. 3) represents the residual $\delta^{18}O$ signal ($\Delta\delta^{18}O$) (*27*) that can be used to define the oxygen isotopic composition of seawater. The mean oxygen isotopic composition of ambient seawater can be determined with the $\delta^{18}O$ residuals for the austral winters when transient changes in seawater $\delta^{18}O$ are negligible (*28*) and central Great Barrier Reef waters are in equilibrium with the regional ocean. The line of best fit through the winter $\delta^{18}O$ residuals in the fossil coral record defines an enrichment in seawater ^{18}O of 0.47 ± 0.13 per mil, relative to modern values. If the mean oxygen isotopic composition of seawater at the end of the deglaciation was the same as today, there should be no offset of the $\delta^{18}O$ and Sr/Ca curves ($\Delta\delta^{18}O = 0$ per mil) for the fossil coral. The ^{18}O enrichment defined by the winters is not a result of a local decrease in precipitation because the seasonal changes in the $\delta^{18}O$ residuals for the fossil coral show that, like today, runoff from mainland rivers carrying monsoonal rainfall with low $^{18}O/^{16}O$ ratios is restricted to the summer and early autumn (December to May). Furthermore, it is unlikely that changes in ocean circulation could have caused the ^{18}O enrichment. Subthermocline water masses in the tropics have low $^{18}O/^{16}O$ ratios relative to surface waters (*29*), so the imposition of an upwelling oceanic regime in the southwestern Pacific would have the opposite effect. Today, the only place in the Pacific where surface seawater $\delta^{18}O$ approaches values 0.5 per mil higher than in the Great Barrier Reef is beneath the southeast Pacific subtropical high-pressure cell, where evaporation greatly exceeds precipitation (*29*). Advection of this ^{18}O-enriched water to the southwestern Pacific cannot be dismissed, but such a change would require a substantial reorganization of the regional oceanic-atmospheric circulation.

We propose that the ^{18}O enrichment is driven by enhanced surface-ocean evaporation in the southwestern Pacific in response to the higher SSTs at the end of the deglaciation. Today, about 11 sverdrup (1 sverdrup = 10^6 m^3 s^{-1}) of water evaporates from the warm surface of the tropics and subtropics, of which about 1.5 sverdrup is transported by the atmosphere and precipitated poleward of ±40° (*30*). The export to higher latitudes of this small portion of the evaporated water leads to an increase of 0.8 per mil in the $^{18}O/^{16}O$ ratio of surface water of the tropical southwestern Pacific relative to mean ocean water (*29*). The 1°C rise in SST reported here would increase surface-ocean evaporation (*31*), particularly before the onset of the monsoon when SSTs warm beyond 27°C to reach average summer maxima of 29.5°C. Enhanced evaporation is evident in the fossil coral record where the $\delta^{18}O$ residuals become progressively more positive in spring and reach maxima in November to December, immediately before the onset of monsoonal rainfall (Fig. 3). The observed ^{18}O enrichment of surface seawater is consistent with general circulation models showing that the poleward transport of water vapor can increase as the atmosphere warms (*32*). Theoretical and general circulation model studies also indicate that even subtle changes in the distribution of tropical heating, particularly warming off the equator,

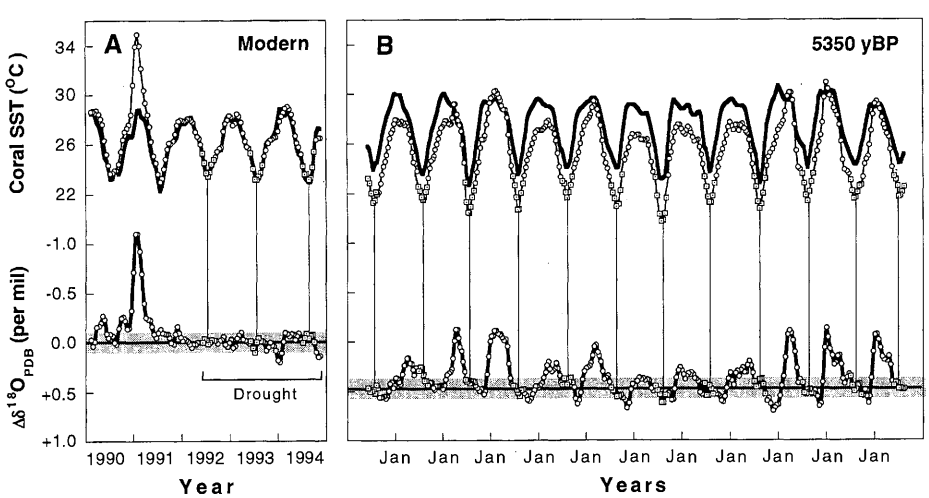

Fig. 3. Comparison between calculated coral Sr/Ca (solid curves) and $\delta^{18}O$ temperatures (upper curves with circles) for the modern (**A**) and 5350 yr B.P. (**B**) *Porites* from Orpheus Island, central Great Barrier Reef. Differences in seawater $\delta^{18}O$ (lower curves with circles), relative to the modern mean, are obtained by removal of the temperature component of the $\delta^{18}O$ signal ($\Delta\delta^{18}O$) (*27*). The horizontal lines show the mean $\Delta\delta^{18}O$ value of seawater for each time-slice, as defined by the seven $\Delta\delta^{18}O$ values (squares) falling in the austral winters (vertical lines). $\Delta\delta^{18}O$ values more negative than the mean define freshening of the ocean surface by ^{18}O-depleted monsoonal rainfall in summer, whereas $\Delta\delta^{18}O$ values more positive than the mean reflect the evaporative ^{18}O-enrichment of the surface ocean in spring. The shaded areas show the uncertainty in estimates of mean $\Delta\delta^{18}O$ (±0.13 per mil, 2σ) on the basis of differences between the data points in Fig. 2B (n = 108) and the mean of the two $\delta^{18}O$–temperature regression lines. The weighted mean regression line used to calculate the $\delta^{18}O$ temperatures is $[\delta^{18}O]_{mean} = 0.146 - 0.179T$ (r = 0.98).

can profoundly alter the intensity of the Hadley circulation and the transport of water vapor and heat into the extratropics (*33*). Although the spatial distribution of the warmer mid-Holocene SSTs needs to be established, it is possible that the equable climates in the extratropical latitudes at this time (*26*) are linked, in part, to an increased latent heat flux from the tropics.

The ^{18}O enrichment of surface seawater identified here may help to reconcile the different temperature histories for the deglacial tropical Pacific given by coral Sr/Ca thermometry and foraminiferal $\delta^{18}O$ records. Taken together with the 5°C cooling indicated by Sr/Ca paleotemperatures for late-glacial corals from the southwest Pacific (*6*), our results indicate that the full amplitude of the glacial-Holocene temperature change may have been about 6°C. A glacial-Holocene shift in foraminiferal $\delta^{18}O$ of 2.7 per mil is required to accommodate the 1.4 per mil change attributed to the 6°C deglacial warming (*34*) and the 1.3 per mil for the generally accepted meltwater contribution (*11*). However, a recent compilation of the glacial-Holocene shift in foraminiferal $\delta^{18}O$ values for 40 western Pacific sediment cores in the latitude range 20°S to 20°N (*35*) reveals an average shift of only 1.6 ± 0.7 per mil (2σ). The maximum $\delta^{18}O$ shift given by the planktonic foraminifer *Globigerinoides sacculifer* in high-quality cores from the tropical southwestern Pacific, near the Great Barrier Reef, is 1.9 per mil (*35*), which is still 0.8 per mil smaller than the expected shift of 2.7 per mil. The important point is that the 0.5 per mil enrichment in surface water $\delta^{18}O$ revealed by the mid-Holocene coral record would reduce the expected glacial-Holocene shift in foraminiferal $\delta^{18}O$ to 2.2 per mil. Complete reconciliation of the foraminiferal $\delta^{18}O$ and coral Sr/Ca records is achieved if the meltwater contribution is reduced by 0.3 per mil, as indicated by recent $\delta^{18}O$ measurements of pore fluids in deep-sea sediments (*36*).

The final 0.5 per mil change in seawater $\delta^{18}O$ during the late Holocene may not be manifest in the $\delta^{18}O$ record provided by core-top foraminifera, considering that the uppermost late-Holocene sediment is commonly lost during the extraction of deep-sea cores. Even in cores with perfect sediment recovery, more than one-half of the final 0.5 per mil adjustment in seawater $\delta^{18}O$ would be masked in the foraminiferal $\delta^{18}O$ records by the 1.2°C cooling required to bring the mid-Holocene SSTs to modern values.

The reconciliation of the foraminiferal $\delta^{18}O$ and coral Sr/Ca records proposed here suggests that the constraint placed on tropical SSTs by foraminiferal $\delta^{18}O$ should be reassessed, at least for the tropical western Pacific. Changes in tropical SSTs, and the rate of delivery of water vapor to higher latitudes, could produce large and abrupt changes in global climate (*9*) during deglaciation. Our results provide the basis for determining the response of the surface-ocean hydrologic balance to such changes, even in tropical oceanic settings where both temperature and seawater $\delta^{18}O$ change in unexpected ways.

REFERENCES AND NOTES

1. J. Chappell and N. J. Shackleton, *Nature* **324**, 137 (1986); N. J. Shackleton, *Quat. Sci. Rev.* **6**, 183 (1987); J. Chappell *et al.*, *Earth Planet. Sci. Lett.* **141**, 227 (1996).
2. The oxygen isotopic composition of foraminiferal calcite is expressed in per mil where $\delta^{18}O = [(^{18}O/^{16}O)_{sample}/(^{18}O/^{16}O)_{standard}] - 1$.
3. N. J. Shackleton, *Nature* **215**, 15 (1967); W. S. Broecker, *Quat. Res.* **26**, 121 (1986); G. E. Birchfield, *Paleoceanography* **2**, 431 (1987).
4. CLIMAP Project Members, *Geol. Soc. Am. Map Chart Ser. MC-36* (1981).
5. T. P. Guilderson, R. G. Fairbanks, J. L. Rubenstone, *Science* **263**, 663 (1994).
6. J. W. Beck, J. Recy, F. Taylor, R. L. Edwards, G. Cabioch, *Nature* **385**, 705 (1996).
7. D. Rind and D. Peteet, *Quat. Res.* **24**, 1 (1985); M. Stute *et al.*, *Science* **269**, 379 (1995); L. G. Thompson *et al.*, *ibid.*, p. 46.
8. W. S. Broecker, *Paleoceanography* **4**, 207 (1989); F. L. Norton, E. D. Hausman, M. B. McElroy, *ibid.* **12**, 15 (1997).
9. W. Broecker, *Science* **272**, 1902 (1996).
10. S. deVilliers, B. K. Nelson, A. R. Chivas, *ibid.* **269**, 1247 (1995).
11. R. G. Fairbanks, *Nature* **342**, 637 (1989).
12. J. W. Beck *et al.*, *Science* **257**, 644 (1992); Sr/Ca ratios were determined by isotope dilution on a Finnigan MAT 261 thermal ionization mass spectrometer with $^{42-43}Ca$-^{84}Sr tracers. In our laboratory, the $^{42-43}Ca$ double spike and the natural $^{86}Sr/^{88}Sr$ ratios were used to correct for mass fractionation. The reproducibility for coral Sr/Ca is ±0.22% ($n = 50$, 2σ).
13. S. deVilliers, G. T. Shen, B. K. Nelson, *Geochim. Cosmochim. Acta* **58**, 197 (1994).
14. Slabs from corals were cut parallel to the axis of maximum growth and reduced to 2-mm thickness, ultrasonically cleaned, and dried at 40°C. Samples 150 to 350 μm thick were then precisely shaved along a continuous strip of 2 mm by 2 mm in cross-sectional area. Our microsampling procedure was designed to provide a minimum of 50 samples per annual growth increment, despite large differences in the annual extension rate among coral colonies, to ensure that the full range of the annual SST cycle was well defined. Every second sample was analyzed (about 25 samples per year), and these data were routinely filtered with a two-point running mean. For comparison with the coral records, blended ship- and satellite-derived SSTs (*15*) were plotted at the same frequency (26 weekly increments per year) and filtered with a two-point running mean to simulate the coral-derived SSTs. The instrumental SSTs have been regressed to reproduce in situ SST measurements made by ships and buoys (*15*). Buoy measurements of SST are typically made at a depth of 0.5 m, whereas ship measurements may be made as deep as 5 m. Therefore, the coral specimens were all collected from 2 to 3 m below mean low sea level so that they compare well with the satellite retrievals of SST.
15. R. W. Reynolds and T. M. Smith, *J. Climate* **7**, 929 (1994).
16. M. K. Gagan, A. R. Chivas, P. J. Isdale, *Geology* **24**, 1009 (1996).
17. S. V. Smith, R. W. Buddemeier, R. C. Redalje, J. E. Houck, *Science* **204**, 404 (1979).
18. C.-C. Shen *et al.*, *Geochim. Cosmochim. Acta* **60**, 3849 (1996).
19. C. Alibert and M. T. McCulloch, *Paleoceanography* **12**, 345 (1997).
20. Oxygen-isotope analyses were carried out on the same samples by an automated individual-carbonate reaction (Kiel) device coupled with a Finnigan MAT 251 mass spectrometer. Calibration to the Pee Dee belemnite (PDB) is through National Bureau of Standards NBS-19. The reproducibility for coral $\delta^{18}O$ is ±0.06 per mil ($n = 34$, 2σ) for a typical 150-μg sample.
21. The mean annual extension rate of each coral colony was determined for at least 5 years of growth as defined by the distance between annual density bands revealed through x-radiography of coral slabs. Mean annual calcification rates were determined by weighing a known volume of coral skeleton spanning 3 to 5 years of growth and calculating the average coral density per unit time. The average difference between replicate coral density determinations was ±0.02 g cm^{-3}.
22. J. M. Lough and D. J. Barnes, *J. Exp. Mar. Biol. Ecol.* **211**, 29 (1997).
23. M. K. Gagan, A. R. Chivas, P. J. Isdale, *Earth Planet. Sci. Lett.* **121**, 549 (1994); M. K. Gagan and A. R. Chivas, *Geophys. Res. Lett.* **22**, 1069 (1995).
24. The conventional radiocarbon age of the sample (ANU-9923) is 5800 ± 60 yr B.P. [M. Stuiver and H. A. Polach, *Radiocarbon* **19**, 353 (1977)]. The reported radiocarbon age was corrected for the apparent age of local seawater by subtracting 450 ± 35 years from the conventional age [R. Gillespie and H. A. Polach, in *Radiocarbon Dating*, R. Berger and H. E. Suess, Eds. (Univ. of California Press, Berkeley, CA, 1979), pp. 404–421].
25. Special care was taken to obtain comparable data sets by matching closely the growth environments of the modern and fossil corals. For example, the paleo-depth of the fossil coral is well constrained because the tops of open-water micro-atolls grow to about the mean low-tide level. The fossil coral record was extracted from the basal section of the coral core ~1.4 m below mean paleo-low tide, whereas the tops of the modern corals were ~2 m below mean low tide. The coral growth rates are also comparable; the mean annual extension rate (15 mm $year^{-1}$) and calcification rate (1.6 g cm^{-2} $year^{-1}$) for the fossil coral is within the range used to calibrate the modern corals.
26. COHMAP Members, *Science* **241**, 1043 (1988); M. S. McGlone, A. P. Kershaw, V. Markgraf, in *El Niño: Historical and Paleoclimatic Aspects of the Southern Oscillation*, H. F. Diaz and V. Markgraf, Eds. (Cambridge Univ. Press, New York, 1994), pp. 435–462.
27. $\Delta\delta^{18}O = \partial\delta^{18}O/\partial T\,[T_{\delta 18O} - T_{Sr/Ca}]$, where $\partial\delta^{18}O/\partial T$ is the empirically derived temperature-dependent oxygen isotope fractionation (−0.18 per mil per degree Celsius) for the *Porites* investigated in this study and elsewhere (*23*).
28. M. T. McCulloch, M. K. Gagan, G. E. Mortimer, A. R. Chivas, P. J. Isdale, *Geochim. Cosmochim. Acta* **58**, 2747 (1994).
29. H. Craig and L. Gordon, in *Stable Isotopes in Oceanic Studies and Paleotemperatures*, E. Tongiorgi, Ed. (Spoleto, Pisa, Italy, 1965), pp. 9–130; H. G. Ostlund, H. Craig, W. S. Broecker, D. Spencer, *GEOSECS Atlantic, Pacific and Indian Ocean Expeditions. Shorebased Data and Graphics 7* (National Science Foundation, Washington, DC, 1987).
30. W. S. Broecker and G. H. Denton, *Geochim. Cosmochim. Acta* **53**, 2465 (1989); F. L. Norton, E. D. Hausman, M. B. McElroy, *Paleoceanography* **12**, 15 (1997).
31. S. Bony, J.-P. Duvel, H. L. Treut, *Climate Dyn.* **11**, 307 (1995).
32. D. Rind, *J. Atmos. Sci.* **44**, 3235 (1987); D. Rind, R. Goldberg, J. Hansen, C. Rosenzweig, R. Ruedy, *J. Geophys. Res.* **95**, 9983 (1990).
33. A. Y. Hou, *J. Atmos. Sci.* **50**, 3553 (1993); R. S. Lindzen and W. Pan, *Climate Dyn.* **10**, 49 (1994).
34. The oxygen-isotope thermometer for calcite precipitation at tropical temperatures in the planktonic foraminifer *G. sacculifer* is −0.23 per mil per degree Celsius [J. Erez and B. Luz, *Geochim. Cosmochim. Acta* **47**, 1025 (1983)].

35. J. I. Martinez, *Palaeogeogr. Palaeoclimatol. Palaeoecol.* **112**, 19 (1994); ______, P. DeDeckker, A. R. Chivas, *Mar. Micropaleontol.* **32**, 311 (1997).
36. D. P. Schrag, G. Hampt, D. W. Murray, *Science* **272**, 1930 (1996).
37. The along-track scanning radiometer (ATSR) data are supplied by the European Space Agency and have been analyzed by the Rutherford Appleton Laboratory, UK.
38. We thank I. Ward for assistance with coral sample preparation and mass spectrometry; S. Anker, S. Vellacott, P. Walbran, and W. Hantoro for help with collecting corals; and W. Beck, D. Schrag, B. Linsley, D. Battisti, and K. Trenberth for valuable discussions. Financial support was provided by the Australian National Greenhouse Advisory Committee.

3 October 1997; accepted 23 December 1997

Simulated Increase of Hurricane Intensities in a CO_2-Warmed Climate

Thomas R. Knutson,* Robert E. Tuleya, Yoshio Kurihara

Hurricanes can inflict catastrophic property damage and loss of human life. Thus, it is important to determine how the character of these powerful storms could change in response to greenhouse gas–induced global warming. The impact of climate warming on hurricane intensities was investigated with a regional, high-resolution, hurricane prediction model. In a case study, 51 western Pacific storm cases under present-day climate conditions were compared with 51 storm cases under high-CO_2 conditions. More idealized experiments were also performed. The large-scale initial conditions were derived from a global climate model. For a sea surface temperature warming of about 2.2°C, the simulations yielded hurricanes that were more intense by 3 to 7 meters per second (5 to 12 percent) for wind speed and 7 to 20 millibars for central surface pressure.

Greenhouse gas–induced climate warming could affect hurricanes in a number of ways, including changing their intensity (*1*, *2*), frequency (*3–5*), and locations of occurrence. Given the potential for catastrophic damage and loss of life from these storms, any such changes could have important societal consequences. In this study, we examine only the question of possible changes in storm intensity due to climate warming.

Theoretical models of hurricane intensity predict that the maximum potential intensity (MPI) of hurricanes will increase in a warmer climate (*1*, *2*), although these techniques, which are based on thermodynamical considerations, contain many assumptions and caveats (*2*, *6*, *7*). Global climate models attempt to simulate the climate, including tropical storm–like features, by integrating dynamical and thermodynamical equations in three dimensions. To date, global models have provided suggestive, but not highly convincing, indications of increased hurricane intensities in a warmer climate (*3*, *4*). However, the coarse resolution of these global models precludes their simulation of realistic hurricane structure. A 1995 assessment by the Intergovernmental Panel on Climate Change (*8*) concludes that ". . . it is not possible to say whether the . . . maximum intensity of tropical cyclones will change" because of increased greenhouse gas concentrations. In the present study, the relation between hurricane intensity and climate change was explored with a regional, high-resolution, hurricane prediction model. We focused on the northwest tropical Pacific region, where the strongest typhoons (the term used in the northwestern Pacific for hurricanes) are observed in the present climate.

In our case study approach, we selected 51 tropical storm cases from a control climate simulation of a global climate model and 51 cases from a high-CO_2 climate simulation (*9*). The global model used was the Geophysical Fluid Dynamics Laboratory (GFDL) R30 coupled ocean-atmosphere climate model (*10–12*), which has resolution of about 2.25° latitude by 3.75° longitude. For the high-CO_2 cases, we selected storms from years 70 to 120 of a +1%-per-year CO_2 transient experiment, corresponding to CO_2 increases ranging from a factor of 2.0 to 3.3. Tropical storm–like features (weaker and much broader than in real-world storms) have previously been analyzed in an R30 global atmospheric model very similar to that used here (*5*, *13*). The selected storm cases were then rerun as 5-day "forecast" experiments with the use of the high-resolution GFDL Hurricane Prediction System (*14*), which is currently used at the U.S. National Centers for Environmental Prediction (NCEP). This model has a maximum resolution in the storm region of 1/6° or about 18 km (*15*). Before beginning each hurricane model simulation, the crudely resolved global model storm (but not the background environment) was filtered from the global model fields and replaced by a more realistic initial vortex (*16*, *17*). This initial vortex replacement procedure is analogous to that used for operational hurricane prediction at NCEP. The storm intensity distributions of the control and high-CO_2 case studies were then compared. Sea surface temperatures (SSTs) were held fixed during the hurricane model experiments. The SSTs and initial environmental

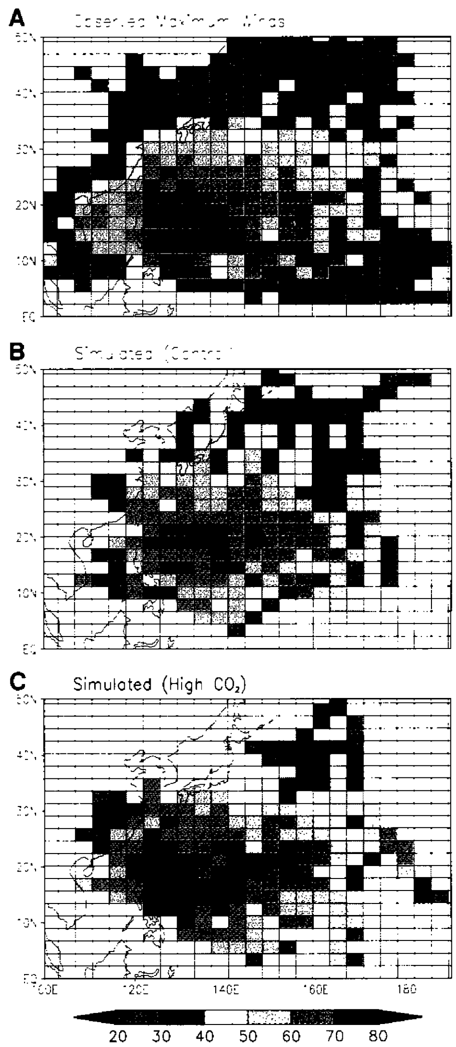

Fig. 1. Geographical distribution of the maximum surface wind speeds (in meters per second) observed during 1971–1992 (**A**) and simulated (**B** and **C**) for tropical storms in the northwest Pacific basin. Observations are from the Joint Typhoon Warning Center (Guam) as compiled by C. J. Neumann in 1993, available from the National Center for Atmospheric Research at www.scd.ucar.edu/dss (ds824.1). The simulated distributions are based on 71 case studies each under control (B) and high-CO_2 (C) conditions; results from 20 preliminary cases under each condition (9) were included in order to increase spatial coverage. Blank (white) regions denote areas where no tropical storms were reported during 1971–1992 (A) or none occurred in the case studies [(B) and (C)].

Geophysical Fluid Dynamics Laboratory/National Oceanic and Atmospheric Administration, Post Office Box 308, Princeton, NJ 08542, USA.

*To whom correspondence should be addressed. E-mail: tk@gfdl.gov